RSC Medicinal Chemistry

ROYAL SOCIETY OF CHEMISTRY

RESEARCH ARTICLE

View Article Online
View Journal | View Issue

Cite this: *RSC Med. Chem.*, 2025, **16**, 2281

Design, synthesis and evaluation of acetylcholine-antitumor lipid hybrids led to identification of a potential anticancer agent disrupting the CDK4/6-Rb pathway in lung cancer†

Ahmed H. E. Hassan,[abcd] Eun Seo Bae,[e] Youngdo Jeong,[f] Chae Won Ock,[e] Selwan M. El-Sayed,[ag] Minji Kim,[f] Mohamed F. Radwan,[h] Tarek S. Ibrahim,[hi] Jun-Young Cho,[f] Boyoung Y. Park,[fj] Jaehoon Sim,[bcd] Sang Kook Lee*[e] and Yong Sup Lee *[bf]

Received 18th December 2024,
Accepted 5th March 2025

DOI: 10.1039/d4md01007h

rsc.li/medchem

Hybridization of acetylcholine with antitumor lipids (ATLs) was explored to achieve novel potential anticancer agents. The combination with a 2-stearoxyphenyl moiety substantially enhanced the anticancer activity of the acetylcholine hybrids. Compounds **6**, **8**, **9** and **10** exhibited pronounced anticancer activities higher than edelfosine and stPEPC and NSC43067. Compounds **6**, **8**, **9** and **10** also showed broad-spectrum anticancer activity against diverse cancer cells including lung, ovarian, renal, prostate, leukaemia, colon, CNS, melanoma, and breast cancer cells. Compounds **6** and **8** were potent compounds eliciting single digit low micromolar GI_{50} values. Compound **6** was the most potent against non-small cell lung cancer, ovarian cancer, renal cancer, and prostate cancer. Meanwhile, compound **8** was the most potent against leukaemia, colon cancer, CNS cancer, melanoma, and breast cancer. Exploration of the mechanism of action of compound **6** in A549 non-small cell lung cancer cells showed that it triggers cell cycle arrest in the G_0/G_1 phase *via* disruption of the CDK4/6-Rb pathway and induces apoptosis *via* the activation of caspases, upregulation of BAX and cleavage of PARP. Overall, the results present acetylcholine-ATL hybrids **6** and **8** as potential anticancer agents for possible further development.

1. Introduction

According to the WHO's world health statistics 2023, cancer is the second major fatal non-communicable disease (NCD) after cardiovascular diseases, accounting for about 9.3 million global deaths.[1] Therefore, cancer treatment remains a significant focus for researchers as the global burden of cancer continues to increase.[2–7] Despite the global efforts to develop anticancer therapies, the optimum anticancer therapeutic agent has not been achieved yet. Furthermore, the heterogeneity of cancer diseases and evolvement of resistance limit the efficacy of current available therapeutics agents. Hence, there is a crucial need for new therapeutic anticancer molecules to overcome such obstacles.[2,8]

Natural compounds, including primary or secondary metabolites, could have indispensable functions within biological systems. Because of their influential impact on the biological system, natural products also play an important role in drug discovery and development.[9–13] As per their definition, natural products are not limited to compounds produced by plants or microorganisms, but extend to those produced by any living organism including animals such as insects or

[a] *Department of Medicinal Chemistry, Faculty of Pharmacy, Mansoura University, Mansoura, 35516, Egypt*
[b] *Department of Pharmacy, College of Pharmacy, Kyung Hee University, Seoul 02447, Republic of Korea. E-mail: kyslee@khu.ac.kr*
[c] *Department of Regulatory Science, Graduate School, Kyung Hee University, Seoul 02447, Republic of Korea*
[d] *Institute of Regulatory Innovation through Science, Kyung Hee University, Seoul 02447, Republic of Korea*
[e] *Natural Products Research Institute, College of Pharmacy, Seoul National University, Seoul 08826, Republic of Korea. E-mail: sklee61@snu.ac.kr*
[f] *Department of Fundamental Pharmaceutical Sciences, Kyung Hee University, Seoul 02447, Republic of Korea*
[g] *Department of Medicinal Chemistry, Faculty of Pharmacy, Mansoura National University, Gamasa 7731168, Egypt*
[h] *Department of Pharmaceutical Chemistry, Faculty of Pharmacy, King Abdulaziz University, Jeddah 21589, Saudi Arabia*
[i] *Department of Pharmaceutical Organic Chemistry, Faculty of Pharmacy, Zagazig University, Zagazig 44519, Egypt*
[j] *Department of Biomedical and Pharmaceutical Sciences, Kyung Hee University, Seoul 02447, South Korea*

† Electronic supplementary information (ESI) available. See DOI: https://doi.org/10.1039/d4md01007h

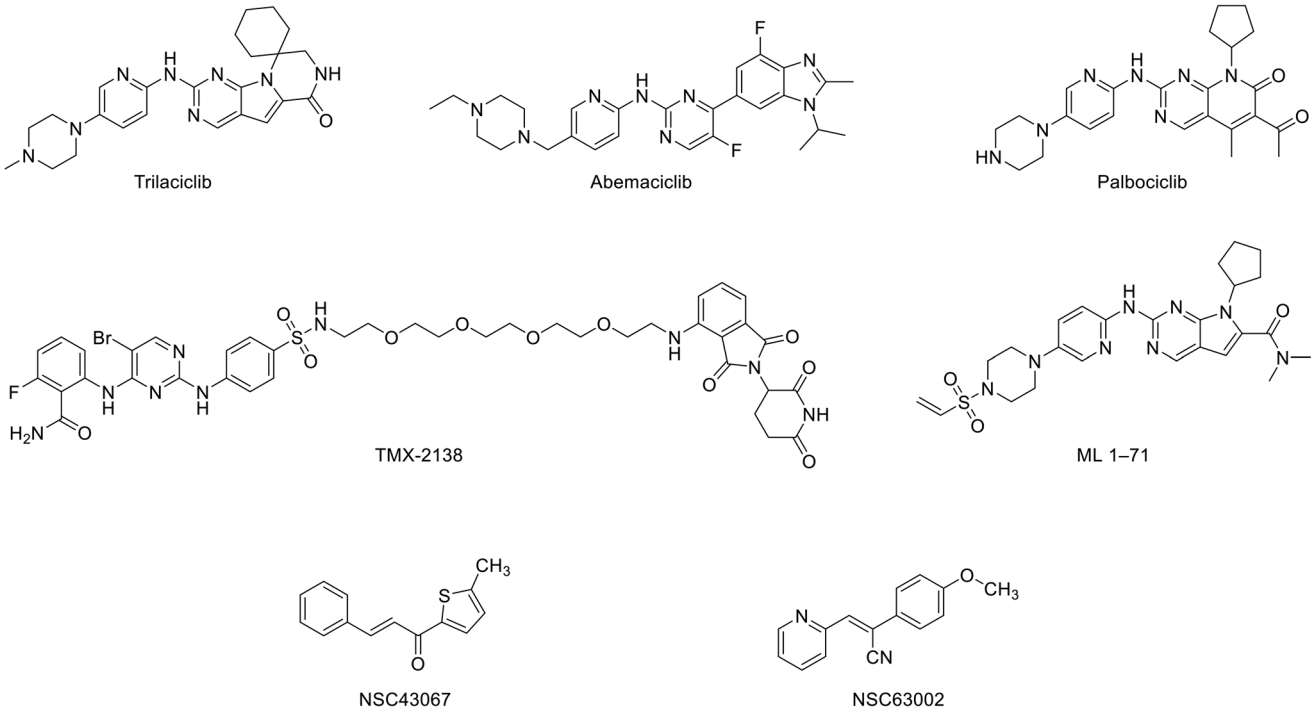

Fig. 1 Examples of literature-known compounds belonging to different categories of compounds targeting CDKs.

mammals. Despite lipids having received relatively low attention, they are among the promising natural products for drug discovery and development.[14–16] Although they are primarily recognized as structural building units, such as lipids in cell membranes or as a mean for energy storage in the body, lipids such as fatty acids, eicosanoids and phospholipids play essential roles in biological functions including cellular regulation and signalling.[17,18] In fact, bioactive lipidic molecules can control and alter health and disease.

Cyclin-dependent kinases such as CDK4 and CDK6 are key players controlling the cell cycle of proliferating cells and, hence, are interesting targets for cancer therapy, including lung cancer and others. Developing therapeutics targeting CDKs can be achieved through developing inhibitor molecules that bind to and prevent the activity of CDKs. In this regard, several heterocyclic scaffolds have afforded CDK inhibitors, such as trilaciclib, palbociclib, and abemaciclib (Fig. 1).[19] Cellular reduction or depletion of the target CDK

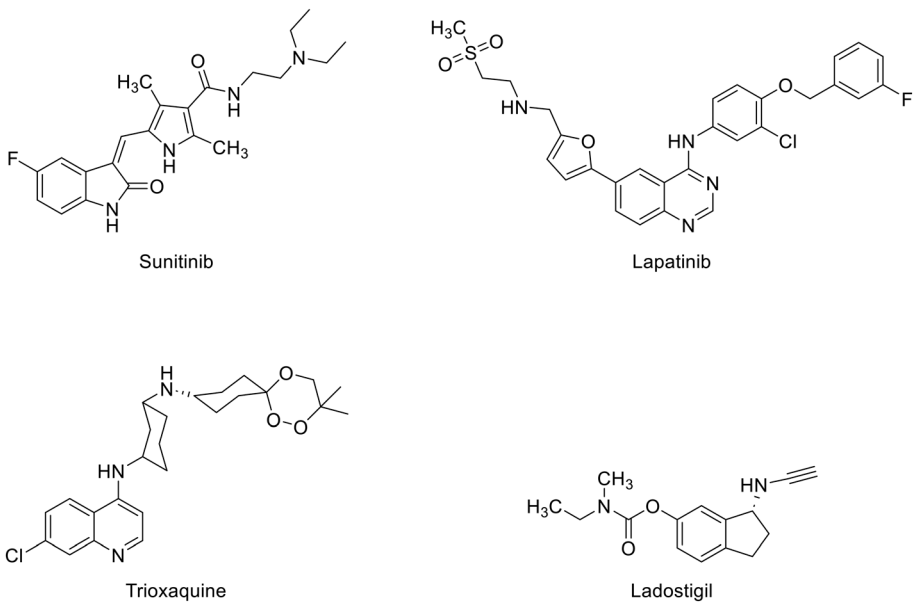

Fig. 2 Examples of successful reports of the development of hybrid drugs.

protein levels through induction of protein degradation using PROTAC or molecular glue degraders, such as TMX-2138 or ML 1–71, respectively (Fig. 1), is an alternative strategy.[20,21] In addition, some compounds inducing CDK protein aggregation, such as NSC43067 and NSC63002, were discovered as a novel class of compounds reducing the cellular levels of CDKs (Fig. 1).[22]

Among the successful drug design techniques is the hybridization approach.[23–30] Compounds designed by this strategy inherit some structural features from parent molecules.[31] Hence, they might elicit bioactivity *via* combining more than one pathway.[2] This might result in a beneficial higher efficacy and lower resistance evolvement rates. Several reports have reported successful stories for this approach for the development of therapeutics against various diseases. Successful examples of such developed hybrid drugs that reached markets include sunitinib, lapatinib, ladostigil, and trioxaquine (Fig. 2).[32]

Among cancer diseases, lung cancer shows the highest incidence and mortality rates.[33–35] This might be contributed by the fact that more than 85% of lung cancer cases are non-small lung cancers, which are less responsive to therapy and furthermore insidious and mostly diagnosed in advanced stages. In combination with the fact that resistance to currently used anticancer agents could evolve, these factors render lung cancer one of the most difficult cancers to treat with poor prognosis and low survival rates. Together, these factors raise urgent needs to discover and develop new anticancer agents against lung cancer and other cancers. In lieu of these needs, we endeavour in the current work to develop new anticancer agents inspired by natural products and following a molecular hybridization approach. Herein, we report our interesting results.

2. Results and discussion

2.1. Design rational

Acetylcholine and its congener butyrylcholine (**1** and **2** respectively, Fig. 3) are natural compounds that are biosynthesized within the body and are well recognized as neurotransmitters. However, they have also other functions including their engagement in oncogenic signalling pathways.[36] It was reported that acetylcholine functions as an autocrine growth factor for lung cancer cell proliferation and acetylcholine signalling modulation impacts the resistance and hinders relapse of EGFR-mutant lung cancer.[37–39] In addition, down-stream targets of acetylcholine are involved in proliferation of various other cancer diseases.[40,41] Due to the reported connection between acetylcholine and cancer, several compounds modulating acetylcholine and butyrylcholine signalling elicit anticancer activity against various cancer diseases.[42–46]

Lysophosphatidylcholines (LysoPCs), such as LysoPC C18:0 (**3**; Fig. 3), are natural compounds biosynthesized through partial hydrolysis of the glycerophospholipids phosphatidylcholines. Investigations of the biological activities of LysoPCs have unveiled their roles in tumour invasion, metastasis and prognosis.[47] In fact, anticancer effects of LysoPCs against several cancers including lung and breast cancers have been reported.[48,49] However, LysoPCs are metabolically labile. Consequently, edelfosine (**4**; Fig. 3), the metabolically more stable analogue of the natural LysoPC C18:0, was developed as a potential anticancer agent.[50–52] Employing edelfosine as a starting point, stPEPC (**5**; Fig. 3) was recently developed as an anticancer agent *via* replacing the central glycerol moiety by a phenethyl moiety.[14,53] In the search for more promising anticancer agents, a molecular hybridization approach was implemented herein to design the targeted derivatives of phenylacetylcholine analogues (**6**; Fig. 3). Thus, the designed derivatives of phenylacetylcholine analogues (**6–23**) incorporate an acetylcholine or acetylcholine-like moiety instead of the methylphosphocholine fragment of LysoPC (**3**) and edelfosine (**4**) or ethylphosphocholine fragment of stPEPC (**5**). Meanwhile, replacement of the central moiety of LysoPC (**3**) or edelfosine (**4**) by an aromatic phenyl ring-containing moiety was maintained in analogy to stPEPC (**5**). While the central glycerol moiety is conformationally flexible, the phenyl ring in the designed derivatives of phenylacetylcholine analogues (**6–23**) can serve as a conformational lock and thus *o*-, *m*-, or *p*-positional scanning of the C18 alkoxy substituent at the phenyl ring might be beneficial. Therefore, restricting the flexibility near the head and such positional scanning were applied in the designed molecules to evaluate their effect regarding biological activity. Furthermore, variation of the quaternary trimethylammonium moiety within the designed derivatives of phenylacetylcholine analogues (**6–23**) by the more steric triethylammonium or cyclic moieties was evaluated. Finally, replacing the two-carbon chain choline moiety by its homologous homocholine moiety that has a longer three-carbon chain was explored.

2.2. Chemical synthesis

Straightforward and concise synthesis of the targeted compounds was achieved in five linear steps employing commercially available hydroxyphenylacetic acid derivatives **24–26** (Scheme 1). The initial step involved esterification to access methyl ester derivatives **27–29**. Thus, methanolic solutions of starting materials **24–26** were treated with acetyl chloride to generate *in situ* hydrochloric acid that promoted an acid-catalysed esterification reaction. The conversion into methyl esters was elucidated by the appearance of a methyl group NMR peak as a singlet within the 3.77–3.72 ppm range in the isolated products **27–29**. The second step involved *O*-alkylation of the phenolic hydroxyl group to access the corresponding stearoxy derivatives **30–32**. This was performed using stearyl tosylate in a nucleophilic substitution reaction in the presence of a catalytic amount of potassium iodide. The conversion into stearoxy derivatives was elucidated by the appearance of NMR peaks in the 3.96–3.93, 1.78–1.73, 1.47–1.24, and 0.89–0.87 ppm ranges corresponding to a

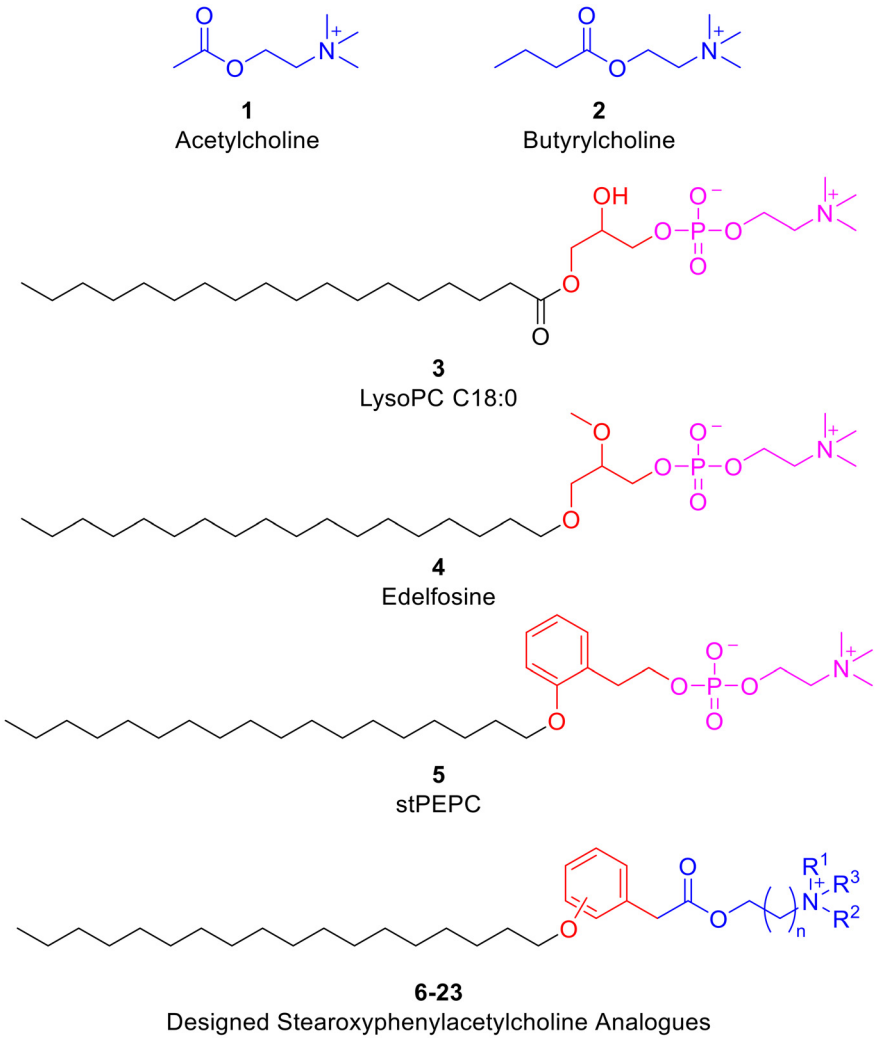

Fig. 3 Previously known bioactive compounds and the design rational of the targeted derivatives of phenylacetylcholine analogues.

stearoxy moiety. The third step was hydrolysis into acid derivatives **33–35** in preparation for choline-like moiety installation in the following steps. Next, installation of the choline-like moieties was started by esterification with appropriate alkanolamines to access ester derivatives **36–53**. This was performed *via in situ* generation of Vilsmeier reagent using stoichiometric oxalyl chloride and catalytic DMF to convert the acid derivatives **33–35** into acid chlorides, which were reacted with the appropriate alkanolamine to afford derivatives **36–53**. The conversion into aminoalkyl esters was elucidated by the appearance of NMR peaks corresponding to the aminoalkyl moieties. For example, compound **36** showed two triplets at 4.22 and 2.58 ppm, each equivalent to methylene protons, in addition to a singlet at 2.27 ppm equivalent to six protons of the two methyl groups. Finally, the aminoalkyl esters **36–53** were converted into the targeted choline analogue derivatives **6–23** *via* quaternization of the tertiary amino nitrogen through stirring their solutions with the appropriate alkyl iodide. The conversion was confirmed by the increase in the chemical shift of protons on the carbons attached to the quaternary nitrogen atom and NMR peak of the introduced alkyl moiety. For example, the chemical shift of the NMR peaks of the methyl and methylene protons of compound **6** increased to 3.04 and 3.62 ppm, respectively, in comparison with 2.27 and 2.58 ppm for the precursor compound **36**. The analytical and spectroscopical data of the synthesized target compounds were in agreement with the expected values, which elucidated their structures.

2.3. Biological evaluations

2.3.1. Anticancer activity against lung cancer cells. Lung cancer is the leading cause of death among all cancer diseases. In fact, lung cancer is a group of heterogenous tumours that originate within lung tissues. In addition to constituting 85% of all lung cancers, non-small cell lung cancer (NSCLC) is less responsive to chemotherapy and more difficult to treat in comparison with small cell lung cancer (SCLC). NSCLC involves heterogenous classes of tumours and

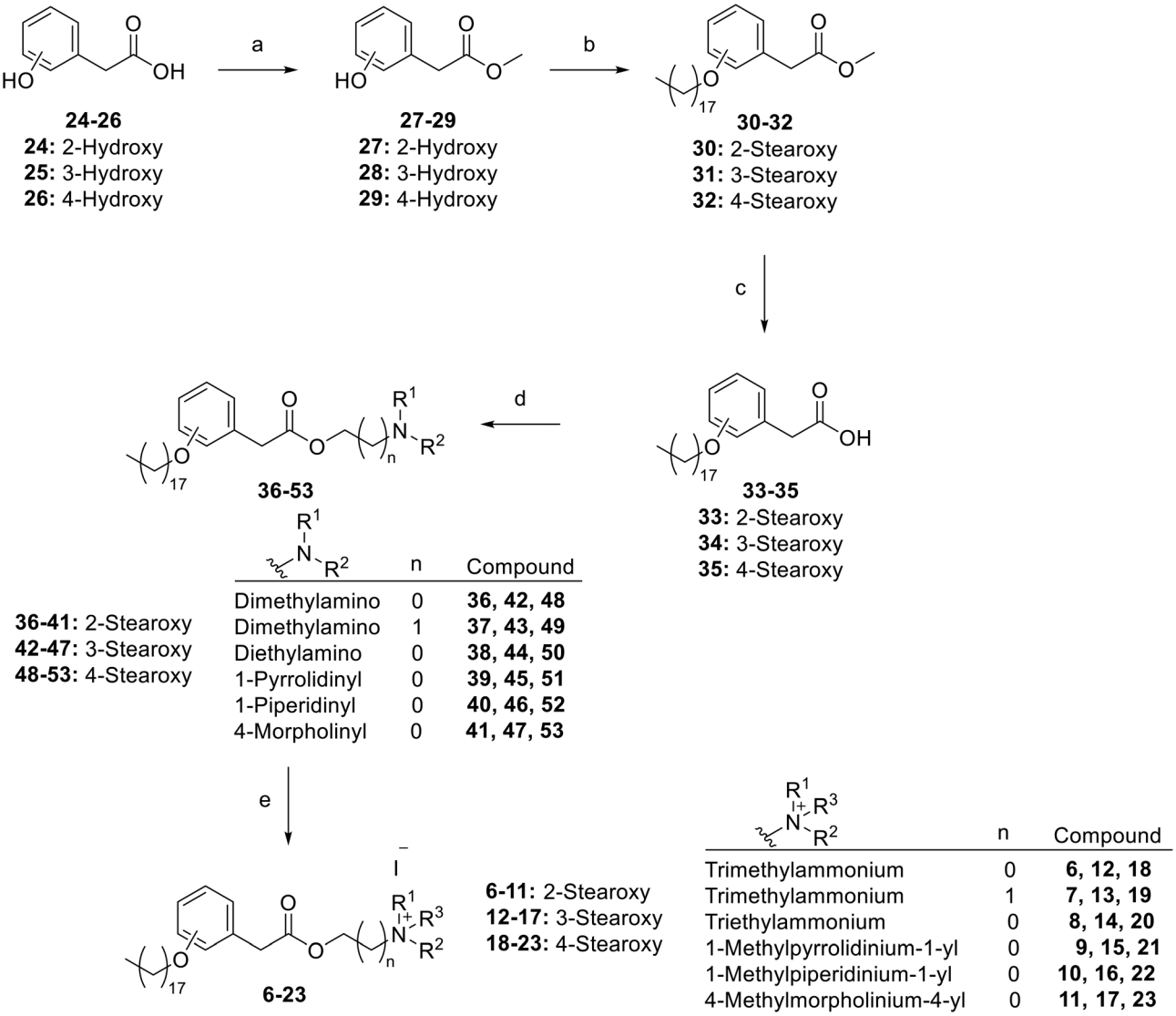

Scheme 1 Synthesis of the targeted derivatives of phenylacetylcholine analogues: a) acetyl chloride, MeOH, 65 °C, 2 h; b) stearyl tosylate, K_2CO_3, cat. KI, DMF, 60 °C, 20 h; c) NaOH, THF, MeOH, 80 °C, 3 h; (d) 1) oxalyl chloride, cat. DMF, anhydrous CH_2Cl_2, 25 °C, 3 h, 2) alkanolamine, CH_2Cl_2, 25 °C, 12 h; (e) alkyl iodide, acetonitrile, ethyl acetate, 25 °C, 24 h.

might be categorized into adenocarcinoma, metastatic adenocarcinoma, large cell carcinoma and squamous carcinoma. Consequently, nine diverse NSCLC cell lines belonging to these categories were employed to get better insights into the activities and efficacies of the synthesized compounds **6–23**. For comparison, compound NSC43067, the edelfosine (**4**) drug and previously reported lead compound stPEPC (**5**) were used as reference standards. The evaluation outcomes are summarized in Table S1† and shown in Fig. 4.

As shown in Fig. 4, the reference compound NSC43067 exhibited low activities at 10 μM concentration against only three cell lines (H460, EKVX, and H522; Table S1†). Meanwhile, both edelfosine and stPEPC at 10 μM concentration, in general, showed modest activity lower than 50% inhibition of NSCLC cell lines. Thus, the average percent inhibition values over the employed 6 adenocarcinoma cell lines, the metastatic adenocarcinoma, and the large cell and squamous carcinomas were 28.03 and 27.69% for edelfosine and stPEPC, respectively. The metastatic adenocarcinoma, the squamous carcinoma and EKVX adenocarcinoma cell lines were the least responsive to both edelfosine and stPEPC (Table S1†). Conversely, the 2-stearoxyphenyl-based series of compounds **6–11** were more active at the tested 10 μM concentration, as shown in Table S1† and Fig. 4. In particular, compound **6** with a calculated value of 77.74% possessed the highest average activity over the tested nine NSCLC cells. It showed its highest activity against NSCLC large cell carcinoma and four out of the tested six NSCLC adenocarcinomas (88.49–114.01% growth inhibition against H460, A549, HOP62, HOP92, and H522 cell lines; Table S1†). In addition, it elicited good activity against NSCLC squamous carcinoma and average activity against two NSCLC

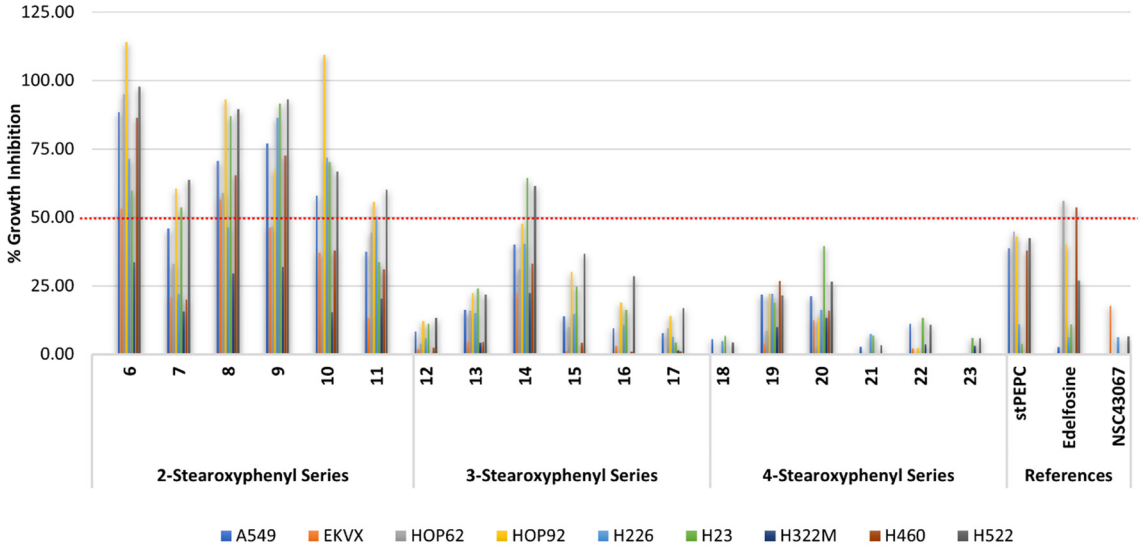

Fig. 4 % Growth inhibition of diverse non-small cell lung cancer cell lines triggered by 10 μM concentrations of the prepared compounds **6**–**23**, stPEPC and edelfosine.

adenocarcinomas (Table S1†). However, it elicited low activity against NSCLC metastatic adenocarcinoma (33.49% growth inhibition; Table S1†). Meanwhile, its homologous compound **7** showed a relatively lower activity than compound **6** but a higher activity than both edelfosine and stPEPC (Table S1†). Thus, compound **7** showed an average activity above 50% against the three NSCLC adenocarcinomas (HOP92, H23 and H522), which is higher than both edelfosine and stPEPC. Nevertheless, the activity of compound **7** was very low against the tested NSCLC metastatic adenocarcinoma, large cell carcinoma, and squamous carcinoma cell lines. Potential anticancer activity was still observed for analogous compounds **8**, **9**, and **10** (Fig. 4). As displayed in Table S1,† compound **8** elicited excellent to average activity against all tested six NSCLC adenocarcinoma cell lines, while the activities of compounds **9** and **10** ranged from excellent to average against four out of the tested six NSCLC adenocarcinoma cell lines (Table S1†). Moreover, compound **8** showed a good activity against NSCLC large cell carcinoma (H460), while compound **10** possessed a good activity against NSCLC squamous carcinoma (H226) and compound **9** was potentially active against both types (Table S1†). Nevertheless, the activities of compounds **8**, **9**, and **10** against metastatic NSCLC adenocarcinoma (H322) were low in a similar pattern to compound **6** and their average growth inhibition values over all tested nine NSCLC cell lines were more than 55% (Table S1†). An exception of the good activity of analogous compounds **6**, **8**, **9**, and **10** was compound **11**, which possessed an average growth inhibition activity over all tested NSCLC cells lower than 40%. It showed growth inhibition of more than 50% against only three NSCLC cells out of the tested NSCLC cells.

Analysis of the results of the 3-stearoxyphenyl and 4-stearoxyphenyl-based series of compounds **12**–**17** and **18**–**23**, respectively, revealed that these two series in general have low activity at the tested concentration (Fig. 4). Among them, only compound **14** showed better activity than the references edelfosine and stPEPC at the tested 10 μM concentration. However, compound **14** was less active than the corresponding 4-stearoxyphenyl-based compound **8**, showing growth inhibition above 50% against only two out of the tested nine NSCLC cells (Table S1†). As Fig. 4 illustrates, the 4-stearoxyphenyl-based series of compounds **18**–**23** were in general even less active than the 3-stearoxyphenyl-based series of compounds **12**–**17**. Together, these results show that the 2-stearoxyphenyl-based compounds **6**–**11** are the most potentially active against diverse NSCLC cells, including NSCLC adenocarcinoma, large cell carcinoma and squamous carcinoma, but not metastatic lung adenocarcinoma. In addition, four compounds (**6**, **8**, **9**, and **10**) out of the 2-stearoxyphenyl-based compounds were found to possess potential activity and might be worth further investigation.

2.3.2. Structure–activity relationship assessment. Analysis of the outcome of the *in vitro* activity evaluation of the synthesised compounds against NSCLC cell lines considering their structures unveiled interesting links between their structures and activity (Fig. 5). The positional relationship between the acetylcholine-like moiety and the stearoxy moiety substituents on the central aromatic phenyl moiety was crucial for the anticancer activity of the compounds. The optimum positional relation was identified to be when substituents are in an *ortho*-positional relationship to each other, while the least active compounds possessed a *para*-positional relationship. The *meta*-positional relationship resulted in compounds much less active than the *ortho*-derived compounds but, in general, having slightly higher activity than the *para*-derived compounds. This was evident clearly from the activity data that presented 2-stearoxyphenyl-based derivatives as the most active, then 3-stearoxyphenyl-based derivatives, and 4-stearoxyphenyl-

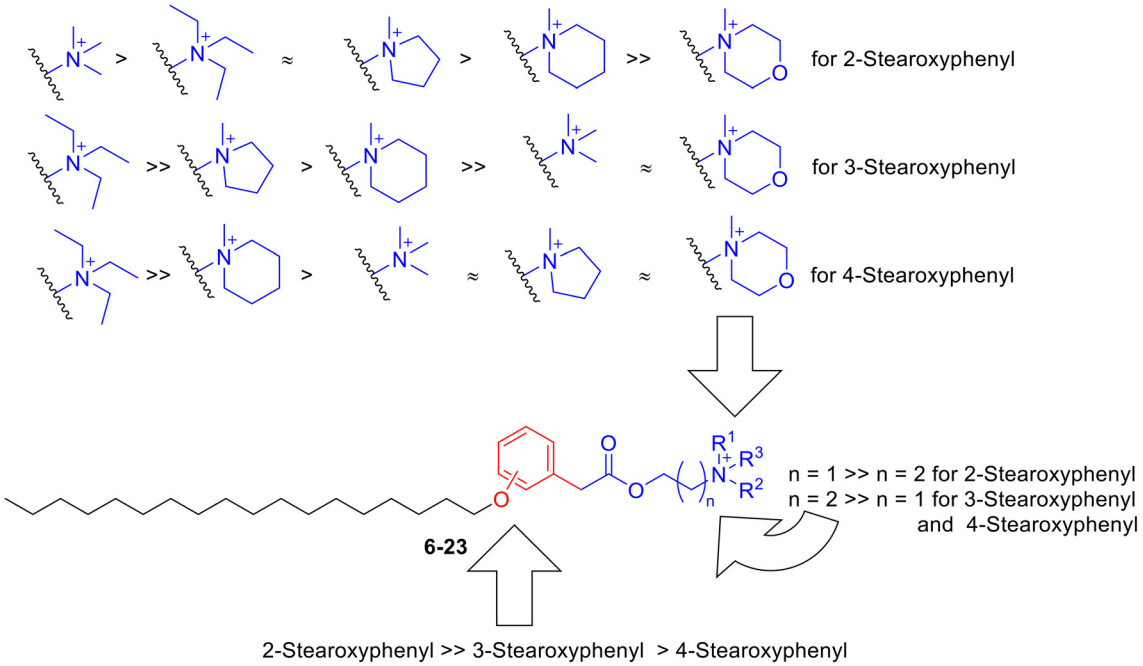

Fig. 5 The relation between structure and anticancer activity of compounds **6**–**23** against human lung cancer.

based derivatives as the least active. Replacing the choline moiety by the homologous homocholine, which has a one-carbon longer chain than choline, resulted in a dramatic decrease of the activity of the 2-stearoxyphenyl-based compounds that have a positional *ortho*-relationship (compound **7** *versus* compound **6**), while it resulted in some increase in activity of the 3- and 4-stearoxyphenyl-based compounds which have positional *meta*- and *para*-relationships (compounds **13** and **19** *versus* compounds **12** and **18**, respectively). Maintaining the two carbon length of the choline chain but tweaking the substituents at the quaternary nitrogen showed that for the 2-stearoxyphenyl-based compounds the trimethyl substituents followed by the triethyl and the cyclic 1-methylpyrrolidinium moieties afforded the most active derivatives (compounds **6**, **8**, and **9**, respectively), followed by the cyclic 1-methylpiperidinium (compound **10**). However, the cyclic 4-methylmorpholinium that has a polar oxygen atom, resulted in deterioration of the activity (compound **11**). While a trimethyl substituent at the quaternary nitrogen afforded the most active compound among the 2-stearoxyphenyl-based compounds, the larger triethyl substituent resulted in the most active compounds within the 3- and 4-stearoxyphenyl-based choline-like containing compounds (compounds **14** and **20**). Interestingly, the 3-stearoxyphenyl-based compounds having 1-methylpyrrolidinium and 1-methylpiperidinium moieties (compounds **15** and **16**) were more active than the trimethylammonium derivative **12**, whose activity was close to that of compound **17**, containing 4-methylmorpholinium. Similarly, the 4-stearoxyphenyl-based compound having a 1-methylpiperidinium moiety (compound **22**) was slightly more active than the trimethylammonium derivative (compound **18**), whose activity was close to the least active compounds **21** and **23** possessing 1-methylpyrrolidinium and 4-methylmorpholinium moieties.

2.3.3. Assessment of the spectrum against diverse cancer cells. The four compounds **6**, **8**, **9** and **10** that were identified as potential anticancer agents against lung cancer were subjected to evaluation of their spectrum as anticancer agents against diverse cancer cells. Fig. 6 shows the results of the evaluations of these four compounds against cell line panels representing multiple cancer diseases, including, in addition to lung cancer, leukemia, colon cancer, CNS cancer, melanoma, ovarian cancer, renal cancer, prostate cancer and breast cancer. As Fig. 6 illustrates, compound **6** showed a broad-spectrum anticancer activity against almost all tested cancer cells. Thus, out of 58 cancer cell lines, compound **6** inhibited the growth of 50 cell lines by more than 50%, including 9 cancer cell lines whose growth inhibition values were more than 100%. Compound **6** elicited a calculated excellent mean growth inhibition value of 81.47% over the 58 cancer cell lines. In addition to its potential activity against lung cancer, compound **6** inhibited all tested leukemia, CNS, prostate and breast cancer cell lines by more than 50%. It showed more than 50% inhibition against 6 out of 7 colon cancer cell lines, 7 out of 9 melanoma cancer cell lines, 5 out of 7 ovarian cancer cell lines, and 6 out of 8 renal cancer cell lines. Like compound **6**, compound **8** elicited broad-spectrum anticancer activity against almost all tested cancer cells. Out of 58 cancer cell lines, compound **8** triggered more than 50% growth inhibition against 49 cell lines, including 10 cells with more than 100% growth inhibition. Compound **8** showed a calculated good mean growth inhibition value of 75.55% over the 58 cancer cell lines. Similar to compound **6**,

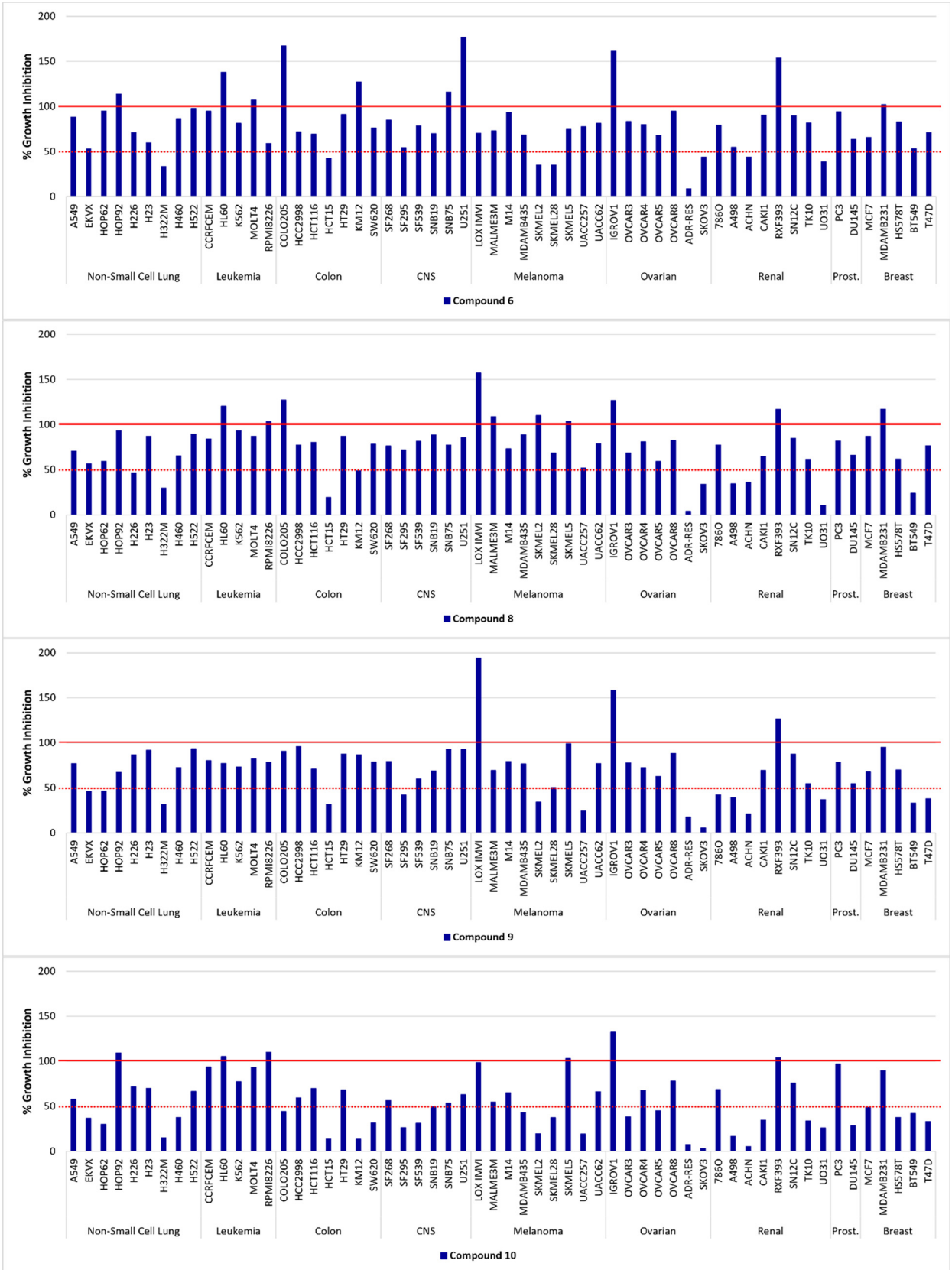

Fig. 6 Evaluation results of the spectrum of anticancer activity of compounds **6**, **8**, **9** and **10** at 10 μM concentration against nine panels of human cancer cells belonging to diverse cancer diseases.

compound **8** inhibited the growth of all tested leukemia, CNS and prostate cancers cell lines by more than 50%. Different from compound **6**, compound **8** was more effective against melanoma but less against breast cancer. Thus, it showed more than 50% growth inhibition of all 9 melanoma cell lines tested, but 4 out of 5 tested breast cancer cells. It inhibited the growth of 6 out of 7 colon cancer cell lines, 5 out of 7 ovarian cancer cell lines, and 5 out of 8 renal cancer cell lines by more than 50%. Although less effective than compounds **6** and **8**, compound **9** had also broad-spectrum anticancer activity against the tested cancer cell panels. Thus, compound **9** inhibited the growth of 43 out of 58 cancer cell lines by more than 50%, including 3 cell lines that were inhibited by more than 100%. Compound **9** exhibited a calculated good mean growth inhibition value of 70.36% over the 58 cancer cell lines. Meanwhile, compound **10** inhibited 31 out of 58 cancer cell lines by more than 50%, including 6 cell lines that were inhibited by more than 100%. Despite its activity over a broad-spectrum of tested cancer cells, compound **10** was the least active among the evaluated four compounds. It possessed a calculated mean growth inhibition value of 55.81% over the 58 cancer cell lines. Together, these results present the four tested compounds as broad-spectrum anticancer agents with different efficacies, where compounds **6**, **8**, and **9** are more effective than compound **10**.

2.3.4. Assessment of anticancer potencies against various cancer cells. The broad-spectrum anticancer compounds **6**, **8**, **9** and **10**, in comparison with edelfosine, the prototype for this class of compounds, were subjected to evaluation of their potencies. In addition to non-small cell lung cancer, determination of their GI_{50} included also leukemia, colon, CNS, ovarian, melanoma, renal, prostate and breast cancers. The results are illustrated in Fig. 7 with an applied cut-off value of 3 μM.

Analysis of the potencies against non-small lung cancer showed that the reference edelfosine possessed GI_{50} values within the range of 7.05–46.77 μM and a calculated average GI_{50} of 25.20 μM; all these values are above the cut-off value of 3 μM for the displayed results in Fig. 7A. Conversely, compound **6** possessed much more superior potencies against all employed cell lines with low GI_{50} values within the range of 1.25–2.17 μM and a calculated average GI_{50} of 1.62 μM. This represents an average 15.5-fold increase compared to the potency of edelfosine. With a calculated average GI_{50} of 1.80 μM and a GI_{50} range of 1.10–4.03 μM, compound **8** possessed excellent potency close to that of compound **6**. Although compounds **9** and **10** elicited much more superior potencies than the reference edelfosine (a calculated average GI_{50} of 2.67 and 2.35 *versus* 25.20 μM and range of 1.22–8.22 and 1.32–5.78 *versus* 7.05–46.77 μM for compounds **9**, **10** and edelfosine, respectively), they were notably less potent than compounds **6** and **8**. Only compound **6** maintained a potent GI_{50} value less than the applied cut-off value against all employed lung cancer cell lines, including the metastatic adenocarcinoma cell line H322M (Fig. 7A). Together, these results suggest consideration of compound **6** as a potential agent against NSCLC for further investigations.

Analysis of the results against four leukemic cancer cells showed that edelfosine possessed GI_{50} values within the range of 3.94–44.26 μM and a calculated average GI_{50} of 16.82 μM. In comparison, all of compounds **6**, **8**, **9** and **10** elicited potencies much superior to edelfosine, showing GI_{50} values less than the applied cut-off value of 3 μM. The most potent was compound **8**, eliciting an average GI_{50} value of 1.29 μM and a range of 0.93–1.50 μM over the used four leukemic cancer cells. This represents an average 13-fold increase compared to the potency of edelfosine. The second most potent was compound **6**, which showed GI_{50} values comparable to those of compound **8**. Compounds **9** and **10** maintained good potencies with GI_{50} less than the applied cut-off value, but were slightly less potent than compounds **8** and **6** as antileukemic agents (Fig. 7B). Based on these results, compounds **8** and **6** might be candidates for further development of antileukemic agents.

The results of potency evaluation against colon cancer cell lines showed than edelfosine elicited GI_{50} within the cut-off value against only two cell lines out of the used seven cell lines (2.38 and 2.65 μM against HCC2998 and COLO205, respectively; Fig. 7C). Over the used seven cell lines, edelfosine showed a calculated average GI_{50} of 7.80 μM and a range of 2.38–14.72 μM. Conversely, compounds **6**, **8**, **9** and **10** were more potent. Among them, only compound **6** maintained GI_{50} values within the applied cut-off value (range of 1.59–2.96 μM) and showed an average GI_{50} value of 1.91 μM. This represents an average 4-fold increase compared to the potency of edelfosine. Although compound **8** showed GI_{50} outside the applied cut-off window against the colon adenocarcinoma HCT15 cell line, it was potent against all other tested colon cancer cell lines showing a calculated average GI_{50} of 1.88 μM and a range of 1.04–4.39 μM. Similarly, compounds **9** and **10** showed GI_{50} outside the applied cut-off window against only the colon adenocarcinoma HCT15 cell line, but were potent against all other tested colon cancer cell lines. Compounds **9** and **10** were of almost equal potencies to each other (average GI_{50} values of 2.17 and 2.16 μM for compounds **9** and **10**, respectively) but, in general, were slightly less potent than compounds **6** and **8**. Collectively, these results present compound **6** as the most promising compound for further development of agents against colon cancer.

Investigation of the potencies against six CNS cancer cell lines showed that edelfosine possessed GI_{50} values above the applied cut-off against all tested cell lines with a calculated average GI_{50} of 21.40 μM and a range of 8.75–58.48 μM. Conversely, all determined GI_{50} values for compounds **6**, **8**, **9** and **10** were within the applied cut-off value (Fig. 7D). Compound **8** was the most potent among the investigated compounds, possessing a calculated average GI_{50} value of 1.35 μM and a range of 0.97–1.62 μM. This represents a more than 15-fold increase compared to the potency of edelfosine. The potencies of the other three compounds **6**, **9** and **10**

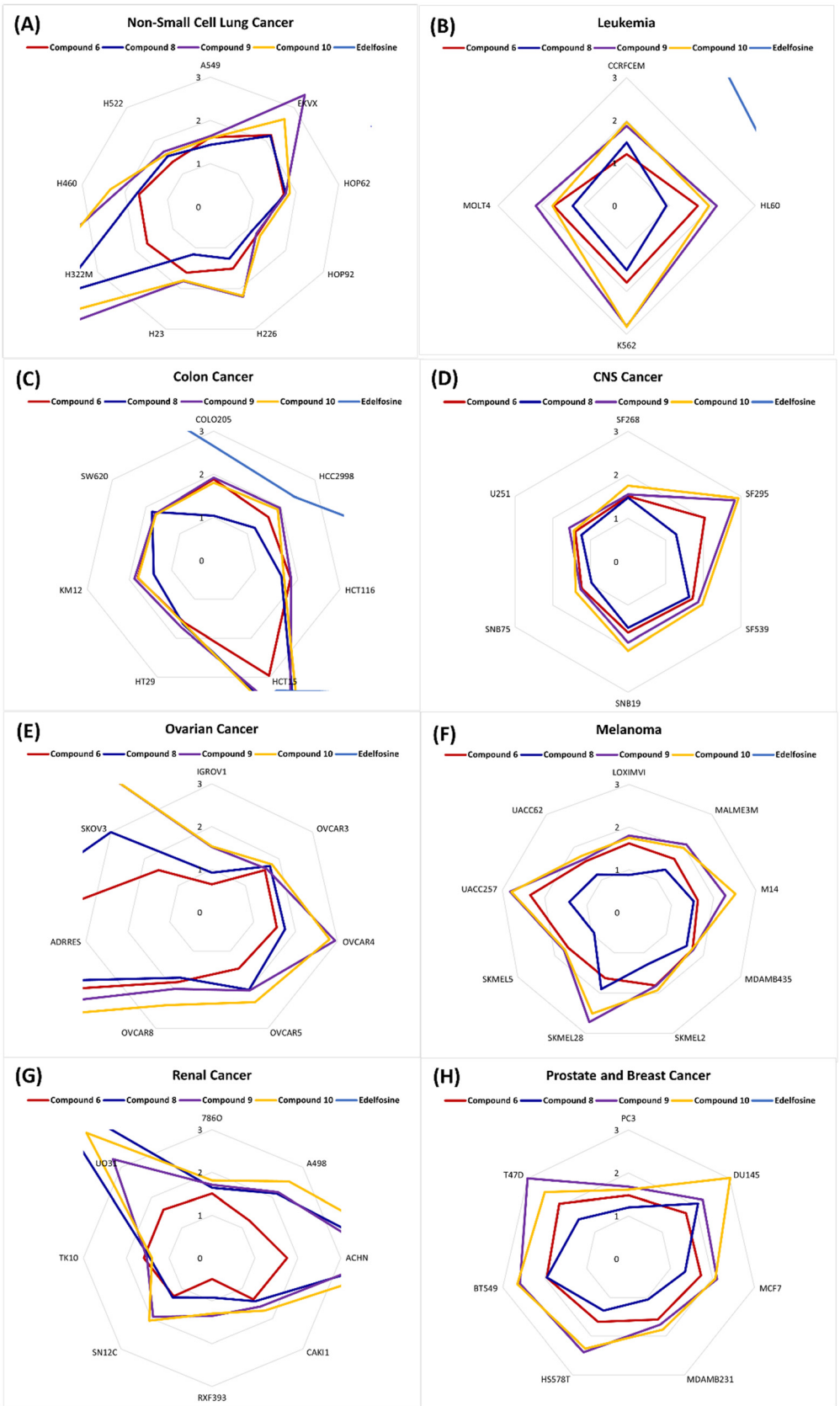

Fig. 7 Results of GI_{50} evaluation for the anticancer activities of compounds **6**, **8**, **9**, **10** and edelfosine against several cancer cells representing diverse cancer diseases: (A) potencies against non-small cell lung cancers; (B) potencies against leukemic cancers; (C) potencies against colon cancers; (D) potencies against CNS cancers; (E) potencies against ovarian cancers; (F) potencies against melanomas; (G) potencies against renal cancers; (H) potencies against prostate and breast cancers.

were, in general, close to each other and to compound **8** (average GI_{50} of 1.59, 1.82, and 1.92 μM with ranges 1.23–2.03, 1.26–2.83, and 1.39–2.93 μM for compounds **6**, **9** and **10**, respectively). Interestingly, compounds **6**, **9** and **10** were less potent against CNS cancer cell line SF295 relative to other CNS cancer cell lines, which is an opposite trend to the determined GI_{50} values of edelfosine where the second best GI_{50} for edelfosine against CNS cancers was against SF295 cells. This might be a reflection of differences between edelfosine and these compounds in their mechanisms of action. Together, these results might nominate compound **8** as the best candidate among the studied compounds as the most promising compound for further development of agents against CNS cancer.

Regarding ovarian cancer, edelfosine possessed GI_{50} outside the applied cut-off, with a GI_{50} range of 6.67–42.27 μM and an average of 25.15 μM. Edelfosine showed its highest potency against the ovarian IGROV1 cell line and least potency against the doxorubicin-resistant ovarian ADRRES cell line. Compounds **6** and **8** possessed similar activity patterns, but with higher potencies (Fig. 7E). The most potent was compound **6** possessing a calculated average GI_{50} of 2.64 μM with a range of 0.65–9.84 μM. This represents a 9.5-fold increase compared to the potency of edelfosine. Close to compound **6** was compound **8** as the second most potent, eliciting a calculated average GI_{50} of 2.67 μM with a range of 0.92–7.58 μM. Compounds **9** and **10** were significantly less potent, showing calculated average GI_{50} values of 6.30 and 6.28 μM with a range of 1.52–18.90 and 1.54–18.20 μM, respectively. Furthermore, their activity trend was different from that of edelfosine, as they were least potent against the ovarian cancer SKOV3 cell line, rather than the doxorubicin-resistant ovarian ADRRES cells. These differences suggest variations in the mode of action of these compounds. Collectively, these results present compounds **6** and **8** as the most potent among the tested compounds for further development of agents against ovarian cancer.

Analysis of the potencies against melanoma showed that edelfosine possessed high GI_{50} values against all nine employed melanoma cell lines, which are outside the applied cut-off value. Edelfosine possessed a calculated average GI_{50} of 38.69 μM with a range of 15.38–98.40 μM. Compounds **6**, **8**, **9** and **10** were notably much more potent than edelfosine with all determined GI_{50} values less than the applied cut-off value (Fig. 7F). Compound **8** was identified as the most potent with a calculated average GI_{50} of 1.33 μM and range of 0.88–1.90 μM. This represents an average 29-fold increase compared to the potency of edelfosine. Compounds **6**, **9** and **10** were also potent but with lower potencies than compound **8**, showing calculated average GI_{50} values of 1.73, 2.07, and 2.07 μM and ranges of 1.57–2.34, 1.63–2.82, and 1.70–2.79 μM for compounds **6**, **9** and **10**, respectively. As illustrated in Fig. 7F, these results present compound **8** as a promising candidate for the development of antimelanoma agents.

Assessment of potencies against eight renal cancer cells showed that edelfosine had a calculated average GI_{50} value of 25.02 μM and range of 12.11–72.78 μM. All these values were higher than the applied cut-off value. In contrast, compound **6** showed much superior potencies that were within the cut-off value against all employed renal cancer cell lines (Fig. 7G). Compound **6** possessed a calculated average GI_{50} value of 1.35 μM with a GI_{50} range of 0.49–1.75 μM. This represented an average 18.5-fold increase compared to the potency of edelfosine. Compounds **8**, **9** and **10** were less potent relative to compound **6** showing almost an average half its potency. Furthermore, the GI_{50} values of compounds **8**, **9** and **10** against two renal cancer cell lines, UO31 and ACHN, were more than the applied cut-off value, which reflected their relatively lower potencies. Hence, among the tested compounds, compound **6** might be the best candidate for further development of agents against renal cancer.

The potency evaluation results against two prostate cancer cell lines and five breast cancer cell lines showed that edelfosine has high calculated average GI_{50} values of more than 53.60 and 67.20 μM against prostate and breast cancers, respectively. In comparison, compounds **6**, **8**, **9** and **10** were much more potent than edelfosine (Fig. 7H). Generally, compound **8** was the most potent against breast cancer, while compound **6** was the most potent against prostate cancer. Compound **8** possessed a calculated average GI_{50} value of 1.43 μM against breast cancer, which is around a 47-fold increase compared to the potency of edelfosine. Meanwhile, compound **6** possessed a calculated average GI_{50} value of 1.60 μM against prostate cancer, which is a 33.5-fold increase compared to the potency of edelfosine. Despite being relatively less potent against prostate and breast cancers, the potencies of compounds **9** and **10** were still comparable to the most potent compounds (compound **6** against prostate cancer and compound **8** against breast cancer). From these results, compound **6** might be nominated for further development of potential agents against prostate cancer, while compound **8** might be nominated for further development of potential agents against breast cancer.

2.3.5. Selectivity against normal cells. Given our interest in developing anti-lung cancer agents coupled the results that revealed compound **6** as a potential agent against lung cancer possessing an average GI_{50} of 1.62 μM and a range of 1.25–2.17 μM against lung cancer cell lines, it was interesting to check whether it exerts a selective cytotoxicity or not. Accordingly, the normal human foetal lung fibroblast MRC-5 cell line was used to check for selective cytotoxic activity. Interestingly, compound **6** was found to elicit a GI_{50} value of 16.7 μM against the used normal cells. This might be translated to an average of 10.31 and a range of 7.70–13.36 selectivity index for lung cancer cells rather than normal lung cells.

2.3.6. Mechanistic studies in A549 lung cancer cells. As compound **6** was identified as the most promising agent against lung cancer coupled with the fact that lung cancer is the cancer disease with the highest mortality, it was of our

interest to investigate how compound **6** can trigger the death of lung cancer. Consequently, the impact of compound **6** on lung cancer A549 cells was further investigated.

2.3.6.1 Compound 6 triggers G_0/G_1 cell cycle arrest in A549 lung cancer cells. Cells undergo different phases during the proliferation cycle, and each phase of this cycle is distinguished by having varying quantities of DNA. Quantifying the DNA content per cell using the fluorescent stain propidium iodide enables classification of a population of cells according to their phase of the cell cycle. As a single copy of DNA exists when cells are in the G_0/G_1 phase, a one-fold fluorescence should be measured for cells in this phase. Because two-DNA copies exist when cells are in the G_2/M phase, two-fold fluorescence should be detected for these cells. Meanwhile, DNA is being synthesized by cells in the S phase and, hence, the detected fluorescence is more than one-fold but less than two fold. Using flow cytometric analysis techniques, the cell cycle distributions of A549 lung cancer cells treated with different concentrations of compound **6** were determined and compared (Fig. 8). The results revealed that the counts of cells in G_0/G_1 phase increased dose-dependently, while the counts of cells in the S and G_2/M phases decreased in a dose-dependent pattern. This outcome showed that compound **6** inhibits the proliferation of A549 lung cancer cells *via* arresting the cells in the G_0/G_1 phase and preventing their progression into the next S phase.

*2.3.6.2 Compound **6** induces apoptotic death in A549 lung cancer cells.* According to some literature reports, G_0/G_1 cell cycle arrest can trigger a subsequent apoptosis, which is a programmed death of cells.[54] Meanwhile, some other reports claimed that it can confer resistance against apoptosis.[55] Accordingly, whether compound **6** might trigger apoptosis or not in A549 lung cancer cells was investigated. As shown in

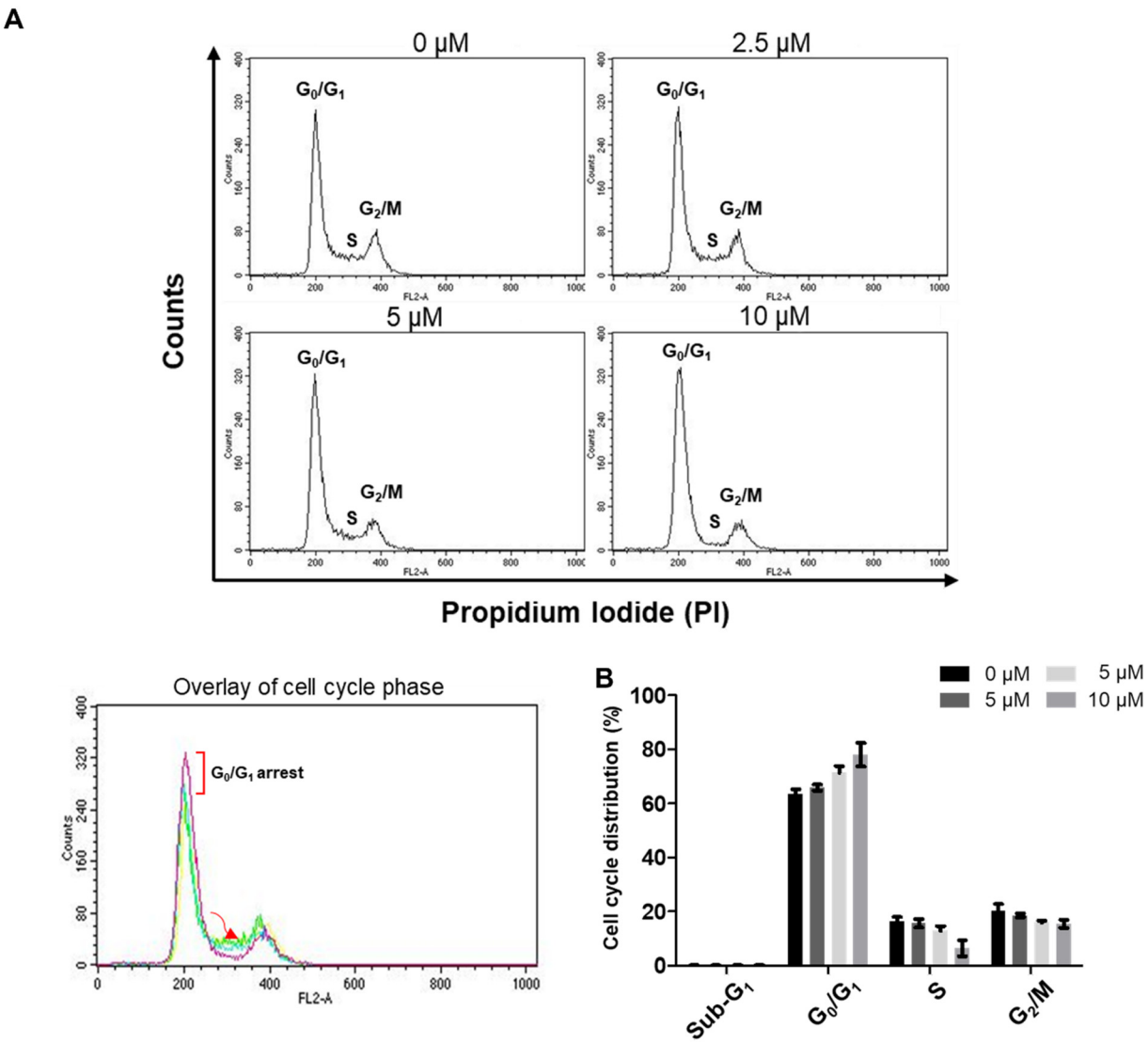

Fig. 8 Changes in cell cycle distributions of A549 cells upon treatment with compound **6**. (A) Flow cytometric analysis of the cell cycle distributions of A549 cells treated with different concentrations of compound **6** after propidium iodide staining. (B) Graphs showing the quantified changes in cell cycle distributions of A549 cells upon treatment with different concentrations of compound **6**.

Fig. 9, fluorescence-activated cell sorting (FACS) flow cytometry post staining with annexin-V and propidium iodide was used to sort A549 cells after treatment with different concentrations of compound **6**. The results showed an increase in the portion of cells that entered the early apoptosis state, and a lower portion entered late apoptosis, while no significant necrosis was detected. The increase in apoptosis was proportional to the employed concentration of compound **6**. It might be concluded that compound **6** triggers G_0/G_1 cell cycle arrest and induces apoptosis in A549 lung cancer cells.

2.3.6.3 G_0/G_1 cell cycle arrest triggered by compound 6 in A549 lung cancer cells is mediated by disruption of the CDK4/6-Rb pathway. To understand the mechanism by which compound **6** triggers G_0/G_1 cell cycle arrest in A549 lung cancer cells, western blotting was performed to investigate proteins involved in cycle regulation that might be responsible for arresting the cells in G_0/G_1 phase. Retinoblastoma (Rb) protein is a tumour suppressor protein that controls the transition from G_1 to S phase in the cell cycle.[56] Phosphorylation of Rb releases the transcription factor E2F from the Rb-E2F complex, prompting the cell to leave G_1 phase and enter S phase.[57] Inhibition of Rb phosphorylation would prevent the cell from entering S phase and eventually arrests the cell in the G_0/G_1 phase. As shown in Fig. 10A, the formation of phospho-Rb (p-Rb) was inhibited dose-dependently. Rb protein is monophosphorylated by cyclin D-CDK4/6, which is further hyperphosphorylated by CDK2. Interestingly, it was reported that the combined loss of CDK2 and CDK4 results in hypophosphorylation of Rb protein.[58] Accordingly, western blotting was performed for CDK2, CDK4, CDK6 and cyclin D1 to investigate their involvement. The results showed dose-dependent inhibition of all these regulator proteins, suggesting that the triggered G_0/G_1 cell cycle arrest by compound **6** is mediated through disruption of the CDK4/6-Rb pathway. Western blotting was also addressed for other CDK isoforms that showed no dose-dependent inhibition of CDK1, CDK7 and CDK8 upon treatment by compound **6** (Fig. S1†). It might be concluded that despite inhibition of CDK4/6 levels mediating the cytotoxic activity of compound **6**, other CDK isoforms including CDK1, CDK7 and CDK8 do not contribute to its cytotoxic activity.

2.3.6.4 Apoptosis triggered by compound 6 in A549 lung cancer cells is mediated via activating the caspase pathway. As the results showed, apoptosis is induced subsequent to G_0/G_1 cell cycle arrest in A549 lung cancer cells by compound **6**. Apoptosis is a programmed cell death that results in DNA fragmentation and cell death.[10,24,33] PARP is a key regulator implicated in DNA repair.[59] Cleavage of PARP results in loss of its function to repair DNA and subsequent DNA fragmentation and apoptosis. Western blotting of PARP and cleaved PARP confirmed that compound **6** induced dose-

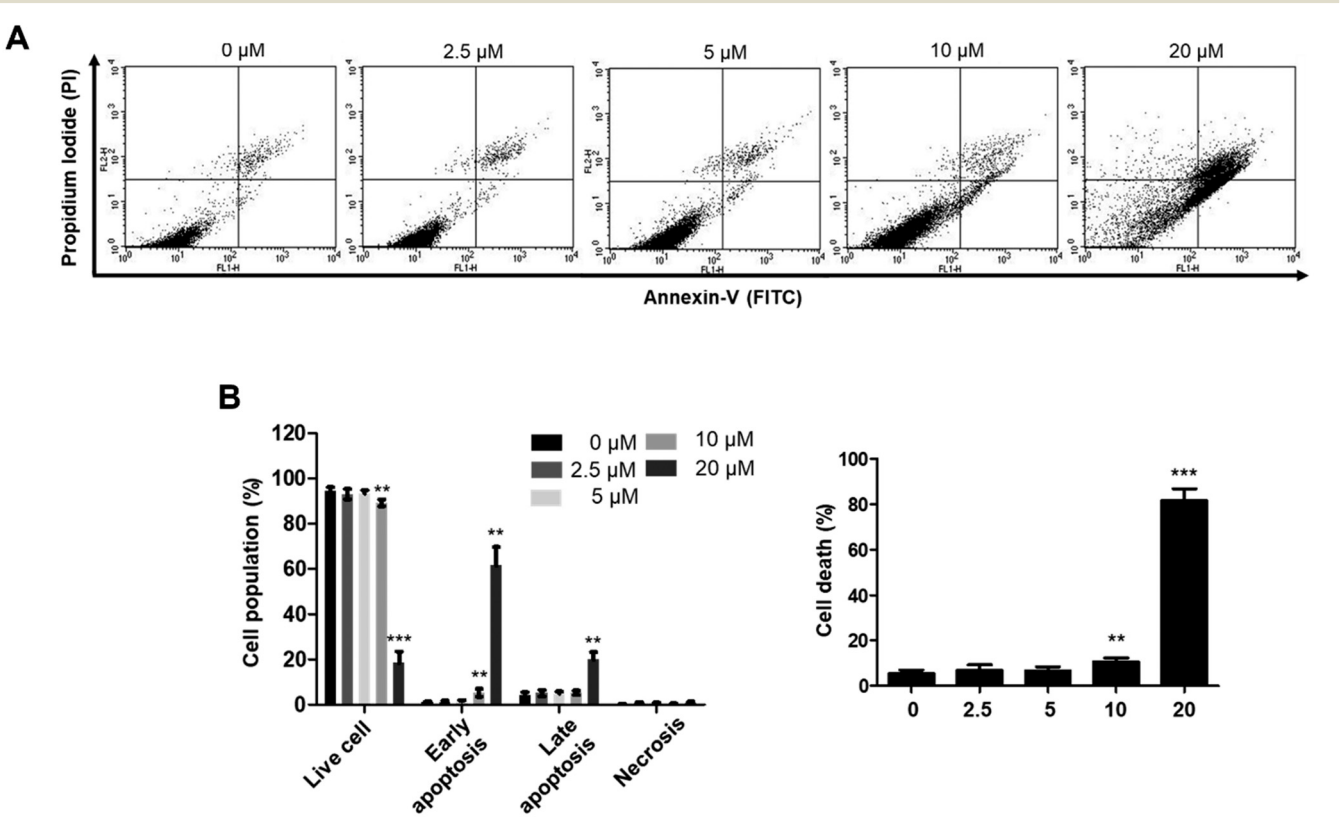

Fig. 9 Apoptosis induction in A549 cells treated with compound **6**. (A) FACS flow cytometric analysis of cell populations treated with different concentrations of compound **6** after annexin-V and propidium iodide staining. (B) The percentages of each cell population (live cell, early apoptosis, late apoptosis, and necrosis) were quantified and presented as a bar graph.

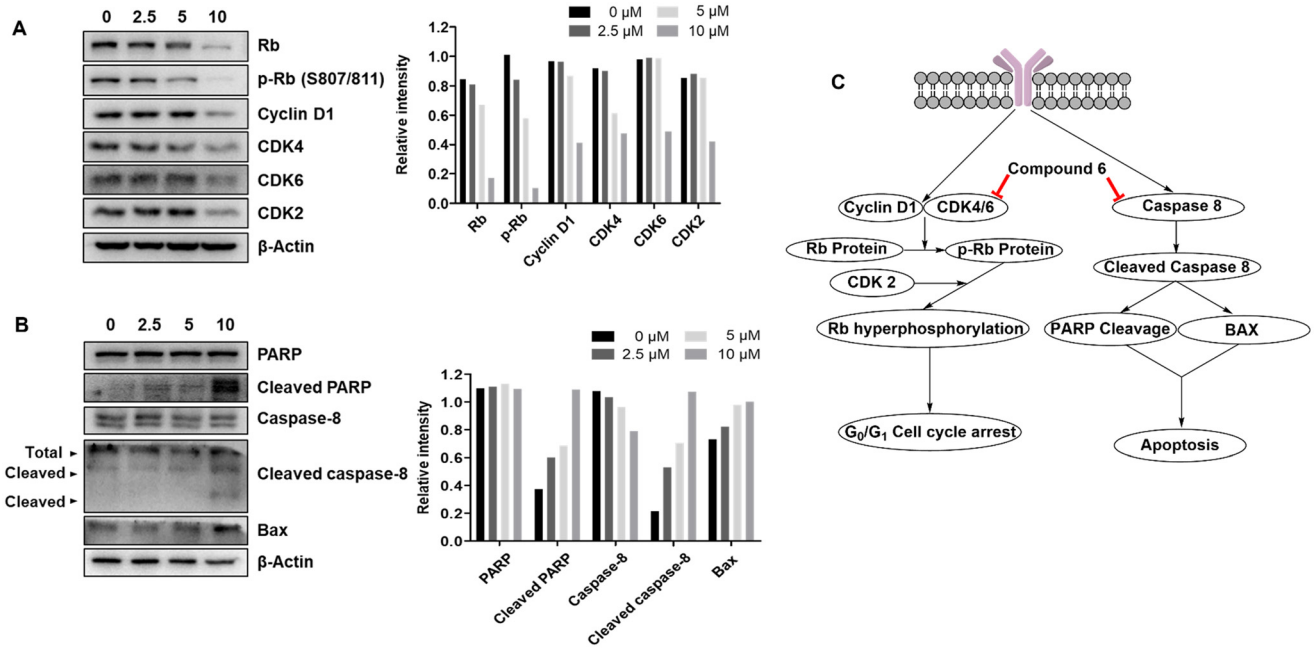

Fig. 10 Western blot analysis of regulatory proteins levels in A549 cells upon treatment with different concentrations of compound **6**. (A) Western blotting and bar representation of quantified regulatory proteins involved in the G_0/G_1 phase of the cell cycle. (B) Western blotting and bar representation of quantified regulatory proteins involved in induction of apoptosis. (C) Schematic representation of pathways contributing to G_0/G_1 cell cycle arrest and induction of apoptosis in A549 lung cancer cells.

dependent PARP cleavage (Fig. 10B). PARP cleavage is a pathway downstream of caspases that includes several members. Among them, caspase 8 is a key member that is involved after cleavage results in activation of other caspases either directly or through upregulation of BAX protein. The latter is a protein that induces opening of mitochondrial voltage-dependent anion channels, loss of mitochondrial potential and further activation of the caspase pathway and eventually PARP cleavage. As shown in Fig. 10, western blots confirmed dose-dependent upregulation of BAX and cleavage of caspase 8 upon treatment with compound **6**. These results suggested that compound **6** induced apoptosis in A549 lung cancer cells through activation of the caspase pathway.

3. Conclusion

Three series of hybrids of acetylcholine derivatives with edelfosine and stPEPC were designed and synthesized. Evaluation of their anticancer activity against a panel of non-small cell lung cancer cell lines showed that compounds belonging to the 2-stearoxyphenyl series were more active than the corresponding compounds from the 3-stearoxyphenyl or 4-stearoxyphenyl series. Four compounds (**6**, **8**, **9** and **10**) were identified as potential inhibitors of non-small cell lung cancer. Further analysis of the spectrum of anticancer activity of compounds **6**, **8**, **9** and **10** against cells representing diverse cancer diseases disclosed their broad-spectrum anticancer activities. Evaluation of their potencies revealed the low micromolar potencies of compounds **6** and **8**. Compound **6** was the most potent against non-small cell lung cancer, ovarian cancer, renal cancer, and prostate cancer. Meanwhile, compound **8** was the most potent against leukemia, colon cancer, CNS cancer, melanoma, and breast cancer. Further evaluation of the mechanism of action of compound **6** in A549 non-small cell lung cancer cells showed that it arrested cells in the G_0/G_1 phase of the cell cycle and induced apoptosis of cells. The triggered cell cycle arrest was mediated *via* disruption of the CDK4/6-Rb pathway, which controls cells' transition from G_1 to S phase, while the induced apoptosis was mediated through activation of the caspase pathway and subsequent upregulation of BAX and cleavage of PARP. Collectively, these results showed that acetylcholine hybrids incorporating a 2-stearoxyphenyl moiety possessed a substantially enhanced anticancer activity and presented acetylcholine hybrids **6** and **8** as potential anticancer agents for possible further development.

4. Experimental section

4.1. Chemistry

Synthesis of the compounds was conducted as detailed in the ESI.†

4.2. Biological evaluation

Biological evaluations were conducted as detailed in the ESI.†

Data availability

All data is included in the manuscript and/or the ESI.†

Author contributions

Conceptualization: A. H. E. H., J. S., S. K. L., and Y. S. L.; data curation: S. K. L. and Y. S. L.; formal analysis: A. H. E. H., E. S. B., Y. J., S. M. E.-S., M. K., M. F. R., and T. S. I.; funding acquisition: J. S., S. K. L., and Y. S. L.; investigation: A. H. E. H., E. S. B., Y. J., C. W. O., M. K., M. F. R., T. S. I., J.-Y. C., and B. Y. P.; methodology: A. H. E. H., J. S., S. K. L., and Y. S. L.; project administration: Y. S. L.; resources: J. S., S. K. L., and Y. S. L.; validation: S. M. E.-S., M. K., and B. Y. P.; visualization: A. H. E. H., E. S. B., Y. J., S. M. E.-S.; all authors contributed to drafting and writing.

Conflicts of interest

There is no conflict of interest to declare.

Acknowledgements

This work was supported by the National Research Foundation of Korea (NRF) grant funded by the Korean government (MSIT) (No. 2021R1C1C1010044). National Cancer Institute, Bethesda, Maryland, USA is acknowledged for performing the NCI-60 human tumour cell line screen. The A549 cancer cell line was obtained from the American Type Culture Collection (Manassas, VA, USA). The MRC-5 cell line was provided by the Korean Cell Line Bank (Seoul, Korea).

References

1 WHO, World Health Statistics 2023. A visual summary, **https://www.who.int/data/stories/world-health-statistics-2023-a-visual-summary/**, (accessed April, 2024, 2024).
2 M. Szumilak, A. Wiktorowska-Owczarek and A. Stanczak, *Molecules*, 2021, **26**, 2601.
3 D. E. Thurston and I. Pysz, *Chemistry and pharmacology of anticancer drugs*, CRC press, 2nd edn, 2021.
4 W. A. Zaki, S. M. El-Sayed, M. Alswah, A. El-Morsy, A. H. Bayoumi, A. S. Mayhoub, W. H. Moustafa, A. A. Awaji, E. J. Roh, A. H. E. Hassan and K. Mahmoud, *Pharmaceuticals*, 2023, **16**, 1593.
5 A. H. E. Hassan, C. Y. Wang, C. J. Lee, H. R. Jeon, Y. Choi, S. Moon, C. H. Lee, Y. J. Kim, S. B. Cho, K. Mahmoud, S. M. El-Sayed, S. K. Lee and Y. S. Lee, *Pharmaceuticals*, 2023, **16**, 1597.
6 A. H. E. Hassan, C. Y. Wang, H. J. Lee, S. J. Jung, Y. J. Kim, S. B. Cho, C. H. Lee, G. Ham, T. Oh, S. K. Lee and Y. S. Lee, *Eur. J. Med. Chem.*, 2023, **256**, 115421.
7 A. K. Farag, A. H. E. Hassan, B. S. Ahn, K. D. Park and E. J. Roh, *J. Enzyme Inhib. Med. Chem.*, 2020, **35**, 311–324.
8 R. Nussinov, C.-J. Tsai and H. Jang, *Drug Resistance Updates*, 2021, **59**, 100796.
9 A. H. E. Hassan, H. J. Kim, S. J. Jung, S.-Y. Jang, S. M. El-Sayed, K.-T. Lee and Y. S. Lee, *Eur. J. Med. Chem.*, 2023, **258**, 115566.
10 J.-H. Won, K.-S. Chung, E.-Y. Park, J.-H. Lee, J.-H. Choi, L. A. Tapondjou, H.-J. Park, M. Nomura, A. H. E. Hassan and K.-T. Lee, *Molecules*, 2018, **23**, 3306.
11 A. H. E. Hassan, K.-T. Lee and Y. S. Lee, *Eur. J. Med. Chem.*, 2020, **187**, 111965.
12 A. H. E. Hassan, H. J. Kim, M. S. Gee, J.-H. Park, H. R. Jeon, C. J. Lee, Y. Choi, S. Moon, D. Lee, J. K. Lee, K. D. Park and Y. S. Lee, *J. Enzyme Inhib. Med. Chem.*, 2022, **37**, 768–780.
13 A. Belal, M. S. Elballal, A. A. Al-Karmalawy, A. H. E. Hassan, E. J. Roh, M. M. Ghoneim, M. A. M. Ali, A. J. Obaidullah, J. M. Alotaibi, S. Shaaban and M. A. Elanany, *Front. Chem.*, 2024, **12**, 1425485.
14 A. H. E. Hassan, Y. I. Oh, C. H. Lee, Y. J. Kim, S. B. Cho, M. M. Alam, S.-E. Park, K.-S. Chung, K.-T. Lee and Y. S. Lee, *J. Enzyme Inhib. Med. Chem.*, 2023, **38**, 2217695.
15 A. H. E. Hassan, H. R. Park, Y. M. Yoon, H. I. Kim, S. Y. Yoo, K. W. Lee and Y. S. Lee, *Bioorg. Chem.*, 2019, **84**, 444–455.
16 M. M. Alam, A. H. E. Hassan, Y. H. Kwon, H. J. Lee, N. Y. Kim, K. H. Min, S.-Y. Lee, D.-H. Kim and Y. S. Lee, *Arch. Pharmacal Res.*, 2018, **41**, 35–45.
17 M. K. Pandey, *Int. J. Mol. Sci.*, 2023, **24**, 13223.
18 J. Park, J. Choi, D.-D. Kim, S. Lee, B. Lee, Y. Lee, S. Kim, S. Kwon, M. Noh, M.-O. Lee, Q.-V. Le and Y.-K. Oh, *Biomol. Ther.*, 2021, **29**, 465–482.
19 S. Lv, J. Yang, J. Lin, X. Huang, H. Zhao, C. Zhao and L. Yang, *Eur. Respir. Rev.*, 2024, **33**, 230145.
20 M. Teng, J. Jiang, Z. He, N. P. Kwiatkowski, K. A. Donovan, C. E. Mills, C. Victor, J. M. Hatcher, E. S. Fischer, P. K. Sorger, T. Zhang and N. S. Gray, *Angew. Chem., Int. Ed.*, 2020, **59**, 13865–13870.
21 M. Lim, T. D. Cong, L. M. Orr, E. S. Toriki, A. C. Kile, J. W. Papatzimas, E. Lee, Y. Lin and D. K. Nomura, *ACS Cent. Sci.*, 2024, **10**, 1318–1331.
22 P. Corsino, N. Horenstein, D. Ostrov, T. Rowe, M. Law, A. Barrett, G. Aslanidi, W. D. Cress and B. Law, *J. Biol. Chem.*, 2009, **284**, 29945–29955.
23 A. H. E. Hassan, C. Y. Wang, T. Oh, G. Ham, S. K. Lee and Y. S. Lee, *Bioorg. Chem.*, 2024, **145**, 107178.
24 J. Y. Hong, K.-S. Chung, J.-S. Shin, J.-H. Lee, H.-S. Gil, H.-H. Lee, E. Choi, J.-H. Choi, A. H. E. Hassan, Y. S. Lee and K.-T. Lee, *Cancers*, 2019, **11**, 1927.
25 A. K. Farag, A. H. E. Hassan, K.-S. Chung, J.-H. Lee, H.-S. Gil, K.-T. Lee and E. J. Roh, *Bioorg. Chem.*, 2020, **103**, 104121.
26 M. M. Alam, A. H. E. Hassan, K. W. Lee, M. C. Cho, J. S. Yang, J. Song, K. H. Min, J. Hong, D.-H. Kim and Y. S. Lee, *Bioorg. Chem.*, 2019, **84**, 51–62.
27 A. H. E. Hassan, E. Choi, Y. M. Yoon, K. W. Lee, S. Y. Yoo, M. C. Cho, J. S. Yang, H. I. Kim, J. Y. Hong, J.-S. Shin, K.-S. Chung, J.-H. Lee, K.-T. Lee and Y. S. Lee, *Eur. J. Med. Chem.*, 2019, **161**, 559–580.
28 A. H. E. Hassan, K. Mahmoud, T.-N. Phan, M. A. Shaldam, C. H. Lee, Y. J. Kim, S. B. Cho, W. A. Bayoumi, S. M. El-Sayed, Y. Choi, S. Moon, J. H. No and Y. S. Lee, *Eur. J. Med. Chem.*, 2023, **250**, 115211.
29 A. H. E. Hassan, W. A. Bayoumi, S. M. El-Sayed, T.-N. Phan, T. Oh, G. Ham, K. Mahmoud, J. H. No and Y. S. Lee, *Pharmaceuticals*, 2023, **16**, 1594.
30 A. H. E. Hassan, W. A. Bayoumi, S. M. El-Sayed, T.-N. Phan, Y. J. Kim, C. H. Lee, S. B. Cho, T. Oh, G. Ham, K. Mahmoud,

J. H. No and Y. S. Lee, *J. Enzyme Inhib. Med. Chem.*, 2023, **38**, 2229071.
31 A. K. Singh, A. Kumar, H. Singh, P. Sonawane, H. Paliwal, S. Thareja, P. Pathak, M. Grishina, M. Jaremko, A.-H. Emwas, J. P. Yadav, A. Verma, H. Khalilullah and P. Kumar, *Pharmaceuticals*, 2022, **15**, 1071.
32 S. Choudhary, P. K. Singh, H. Verma, H. Singh and O. Silakari, *Eur. J. Med. Chem.*, 2018, **151**, 62–97.
33 H.-S. Gil, J.-H. Lee, A. K. Farag, A. H. E. Hassan, K.-S. Chung, J.-H. Choi, E.-J. Roh and K.-T. Lee, *Cancers*, 2021, **13**, 5849.
34 J.-H. Lee, H.-H. Lee, K. D. Ryu, M. Kim, D. Ko, K.-S. Chung, A. H. E. Hassan, S. H. Lee, J. Y. Lee and K.-T. Lee, *J. Clin. Med.*, 2020, **9**, 704.
35 K. C. Thandra, A. Barsouk, K. Saginala, J. S. Aluru and A. Barsouk, *Contemp. Oncol.*, 2021, **25**, 45–52.
36 H. Xu, Z. Shen, J. Xiao, Y. Yang, W. Huang, Z. Zhou, J. Shen, Y. Zhu, X.-Y. Liu and L. Chu, *BMC Cancer*, 2014, **14**, 668.
37 J. R. Friedman, S. D. Richbart, J. C. Merritt, K. C. Brown, N. A. Nolan, A. T. Akers, J. K. Lau, Z. R. Robateau, S. L. Miles and P. Dasgupta, *Pharmacol. Ther.*, 2019, **194**, 222–254.
38 M. Nie, N. Chen, H. Pang, T. Jiang, W. Jiang, P. Tian, L. Yao, Y. Chen, R. J. DeBerardinis, W. Li, Q. Yu, C. Zhou and Z. Hu, *J. Clin. Invest.*, 2022, **132**, e160152.
39 H.-J. Xi, R.-P. Wu, J.-J. Liu, L.-J. Zhang and Z.-S. Li, *Thorac. Cancer*, 2015, **6**, 390–398.
40 A. L. Aronowitz, S. R. Ali, M. D. E. Glaun and M. Amit, *Adv. Biol.*, 2022, **6**, 2200053.
41 H. Yu, H. Xia, Q. Tang, H. Xu, G. Wei, Y. Chen, X. Dai, Q. Gong and F. Bi, *Sci. Rep.*, 2017, **7**, 40802.
42 I. C. Vaaland Holmgard, A. González-Bakker, E. Poeta, A. Puerta, M. X. Fernandes, B. Monti, J. G. Fernández-Bolaños, J. M. Padrón, Ó. López and E. Lindbäck, *Org. Biomol. Chem.*, 2024, **22**, 3425–3438.
43 M. Hudáčová, S. Hamuľaková, E. Konkoľová, R. Jendželovský, J. Vargová, J. Ševc, P. Fedoročko, O. Soukup, J. Janočková, V. Ihnatova, T. Kučera, P. Bzonek, N. Novakova, D. Jun, L. Junova, J. Korábečný, K. Kuča and M. Kožurková, *Int. J. Mol. Sci.*, 2021, **22**, 3830.
44 U. Karmacharya, P. Chaudhary, D. Lim, S. Dahal, B. P. Awasthi, H. D. Park, J.-A. Kim and B.-S. Jeong, *Bioorg. Chem.*, 2021, **110**, 104805.
45 Z. Sun, M. Zhangsun, S. Dong, Y. Liu, J. Qian, D. Zhangsun and S. Luo, *Mar. Drugs*, 2020, **18**, 61.
46 A. Saeed, P. A. Mahesar, S. Zaib, M. S. Khan, A. Matin, M. Shahid and J. Iqbal, *Eur. J. Med. Chem.*, 2014, **78**, 43–53.
47 P. Liu, W. Zhu, C. Chen, B. Yan, L. Zhu, X. Chen and C. Peng, *Life Sci.*, 2020, **247**, 117443.
48 L. Zhang, X. Liu, Y. Liu, F. Yan, Y. Zeng, Y. Song, H. Fang, D. Song and X. Wang, *Clin. Transl. Med.*, 2023, **13**, e1180.
49 D. Mohamad Ali, K. Hogeveen, R.-M. Orhant, T. L. G. de Kerangal, F. Ergan, L. Ulmann and G. Pencreac'h, *Nutrients*, 2023, **15**, 2137.
50 N. P. Tambellini, V. Zaremberg, S. Krishnaiah, R. J. Turner and A. M. Weljie, *J. Proteome Res.*, 2017, **16**, 3741–3752.
51 E. L. H. Dakir, C. Gajate and F. Mollinedo, *Biomed. Pharmacother.*, 2023, **167**, 115436.
52 F. T. Sarah, P. R. Cecilia, J. S. C. Cícero, N. P. Thais, A. D. A. Ricardo, I. M. Lisley, D. J. Salomão, N. R. Rodrigo, S. F. Emer, A. M. B. José and K. F. Adilson, *Anti-Cancer Agents Med. Chem.*, 2018, **18**, 865–874.
53 S.-E. Park, K.-S. Chung, S.-W. Heo, S.-Y. Kim, J.-H. Lee, A. H. E. Hassan, Y. S. Lee, J. Y. Lee and K.-T. Lee, *Life Sci.*, 2023, **334**, 122227.
54 H. Liu, Z. Li, S. Huo, Q. Wei and L. Ge, *Mol. Clin. Oncol.*, 2020, **12**, 9–14.
55 M. Kluska, A. W. Piastowska-Ciesielska and P. Tokarz, *Curr. Issues Mol. Biol.*, 2023, **45**, 6325–6338.
56 A. Sun, L. Bagella, S. Tutton, G. Romano and A. Giordano, *J. Cell. Biochem.*, 2007, **102**, 1400–1404.
57 N. Sobhani, A. D'Angelo, M. Pittacolo, G. Roviello, A. Miccoli, S. P. Corona, O. Bernocchi, D. Generali and T. Otto, *Cell*, 2019, **8**, 321.
58 C. Berthet, K. D. Klarmann, M. B. Hilton, H. C. Suh, J. R. Keller, H. Kiyokawa and P. Kaldis, *Dev. Cell*, 2006, **10**, 563–573.
59 A. Ray Chaudhuri and A. Nussenzweig, *Nat. Rev. Mol. Cell Biol.*, 2017, **18**, 610–621.

